Earthquake Engineering, Tenth World Conference © 1992 Balkema, Rotterdam. ISBN 90 5410 060 5

Surface wave propagation analysis in the Kanto basin

Masato Motosaka, Masaki Kamata & Osamu Sugawara
Kobori Research Complex, Kajima Corporation, Tokyo, Japan

Masanori Niwa
Kajima Technical Research Institute, Tokyo, Japan

ABSTRACT: Surface wave propagation characteristics of the Kanto basin in Japan are investigated analytically based on the geological subsurface structure. First, a 2-dimensional (2D) analysis using the hyper-element method is performed. The observation records in the basin and at its margin due to a shallow earthquake which occurred near the Izu-peninsula are utilized. It is found that only the first major phase of the records is simulated well and it is suggested that the later phases are affected by the 3-dimensional (3D) structure. Next, a 3D analysis is conducted using the simplified 3D-FEM. This method can be applied efficiently in computation to wave propagation problems of a large scale basin. It is found that consideration of 3D subsurface irregularity is important in estimating the long-period ground motions in a basin due to surface waves and it is suggested that the radiation pattern from the source may also be important.

1 INTRODUCTION

For seismic design of large-scale structures such as long- span bridges, high rise buildings, and large tanks, it is important to estimate long-period ground motions, which consist mainly of surface waves. It has been reported that ground motions in a sedimentary basin become larger in amplitude and longer in duration than those at its margins. This is of great engineering concern because many large cities in the world, including Tokyo, are located more or less in a sedimentary basin. The Tokyo Bay area is part of the Kanto basin, as shown in Figure 1. It has been reported that the significant surface waves have been observed during earthquakes occurring near the Izu-peninsula (e.g.Kudo,1978).

The authors have analytically investigated the 2D wave propagation characteristics of the Kanto basin for incident body waves using the discrete wavenumber method and have suggested that the contribution of the surface waves generated at the margin from the body wave to the observation records is small for a shallow earthquake occurring around the Izu-peninsula (Motosaka,1990).

This paper describes the surface wave propagation characteristics of the Kanto basin for incident surface waves using the observation records in the basin and at its margin. 2D and 3D analyses are performed based on the realistic geological subsurface structure .

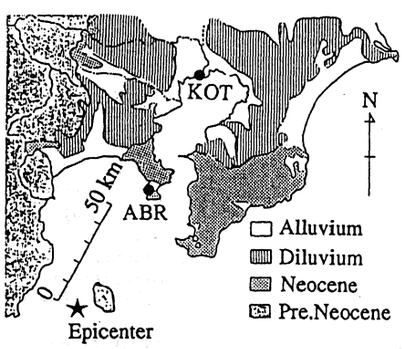

Figure 1. Geological map of the area around the Kanto basin and observation sites

2 ANALYSIS OF OBSERVATION RECORDS

The observation records at Kotoh (KOT) in the Tokyo Bay area of the Kanto basin due to the Feb. 20, 1990 Near Izu-Oshima Earthquake (M=6.5, Depth= 6 km) included long period contents with a predominant period of about 8 seconds and a duration of about 300s, as shown in Figure 2(ref.to Niwa et al.,1990). This figure also shows the particle orbits. It is found from this figure that the long-period contents do not include vertical components, that the principal axis of the particle orbit is perpendicular to the epicentral direction at the beginning of the time history and that the orbits change clockwise with time. This suggests that the long period contents of the ground motion at KOT is the Love wave. Therefore, the transverse component is calculated and compared with that at Aburatubo(ABR), located at the margin of the Kanto basin, as shown in Figure 3. The amplitude of the wave at KOT is two to three times larger and of longer duration than that at ABR, although ABR is located about midway between the epicenter and KOT (ref. to Figure 1).

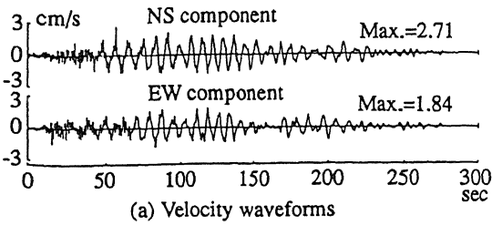

(a) Velocity waveforms

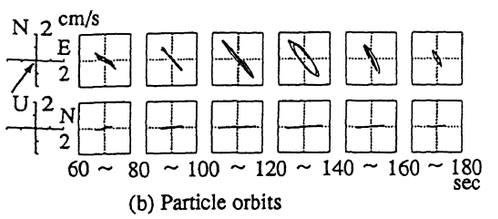

(b) Particle orbits

Figure 2. Observation records and particle orbits at KOT due to the Feb.20 Near Izu-Ohsima Earthquake

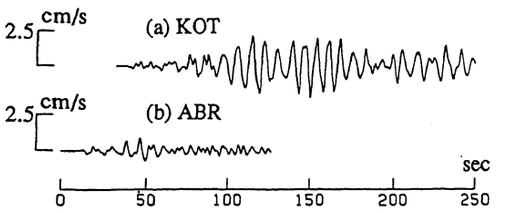

Figure 3. Comparison of waveforms at KOT and ABR (Low-pass filtered waves at 0.4 Hz)

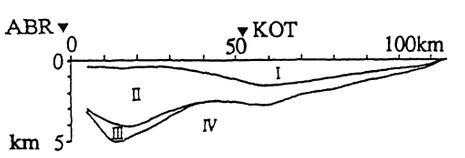

Figure 4. Subsurface structure for the section through KOT and ABR

Table 1. Soil parameters for each layer

Layer	P-wave Velocity km/sec	S-wave Velocity km/sec	Density t/m^3
I	1.83	0.7	2.0
II	2.8	1.3	2.3
III	4.8	2.4	2.5
IV	5.6	2.9	2.5

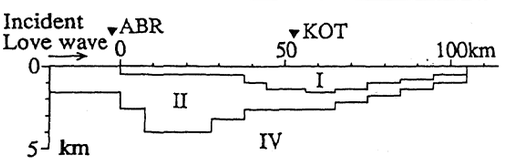

Figure 5. Analytical model of the section by the hyper-element Method

3 2D-WAVE PROPAGATION ANALYSIS

3.1 *Numerical method*

The semi-analytical finite element method (Hyper-element Method, Kausel 1977) was applied to surface wave propagation analysis of the 2D section of the Kanto basin. In this method, the objective irregular structure is modeled by several flat-layered regions comprising different strata. The wave functions are used as an interpolation function in the horizontal direction and a linear interpolation function in the vertical direction. Boundary conditions on the displacements and tractions at the vertical interfaces are satisfied at nodal points of the hyper-element. The mode coupling can be taken into account rigorously.

3.2 *Analytical model*

The SW-NE section of the Kanto basin through KOT and ABR is assumed as shown Figure 4, based on the references (e.g. Yumenoshima explosion tests, Shima,1976). Table 1 shows the soil parameters of each layer in Figure 4. The analytical model by hyper-elements is shown in Figure 5. The quality factor of each layer is assumed to be Vs(m/s)/15, where Vs denotes the shear wave velocity. The objective frequency range is 0-0.4 Hz.

As input waves, a Gabor wavelet (Červeny,1983) and the transverse component of velocity wave at ABR obtained from the acceleration record are used. These waves are assumed to be the fundamental mode of the Love wave.

3.3 *Results and discussions*

Figure 6 shows the synthetic waveforms in the structural model for the Gabor wavelet with a predominant period of 8s. It is recognized from this figure that the incident surface wave is amplified in the sediment of the basin, especially in the region where the top layer becomes thick near KOT, and that the surface wave propagates with the specific group velocity depending on the local soil profile. The phases of the reflected waves are recognized. Figure 7 shows the waveforms for the seismic wave incidence. It is recognized that the waveforms show dispersive characteristics and that the duration becomes longer in the interior part. It is also found that the amplitude of the surface wave becomes larger near KOT.

The observed waveform (low-pass filtered at 0.4Hz) is compared with the synthetic waveform at KOT in Figure 8. The filtered wave at ABR is also shown in this figure. It is found from the figure that the amplitude of the synthetic wave at KOT is smaller than that of the observation records there, although the synthetic wave is amplified 1.5 times in amplitude compared with the observation record at ABR. It is also found that the observed wave group A shown in the figure is comparatively well simulated in this simulation analysis, but that the wave group B is not expressed well.

These results suggest that wave group A propagates along the section of the model from the epicentral distance, but that wave group B is affected by the 3D geological structure of the Kanto basin.

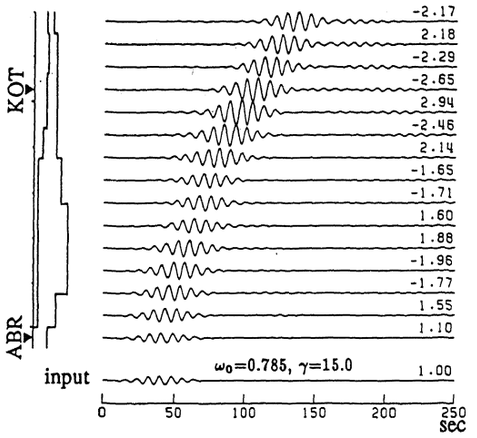

Figure 6. Synthetic waveform in different locations subjected to the Gabor wavelet incidence

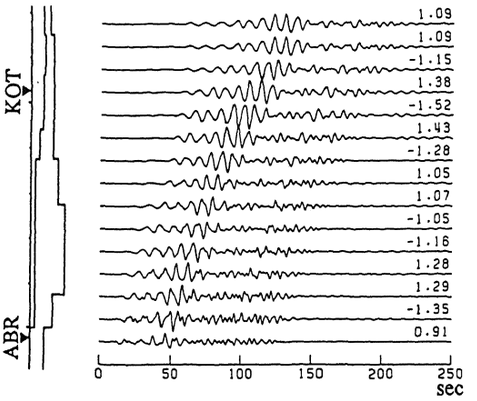

Figure 7. Synthetic waveform in different locations subjected to the observation records at ABR

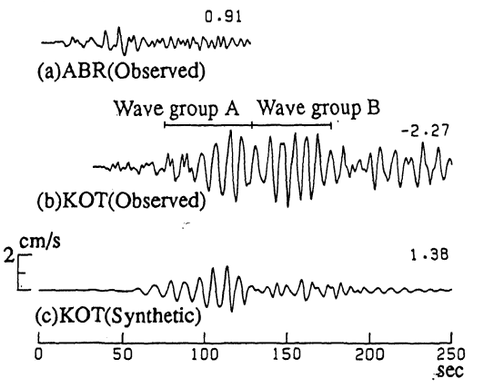

Figure 8. Comparison of observed waveforms with synthetic waveform

4 3D-WAVE PROPAGATION ANALYSIS

4.1 *3D-subsurface structure*

The bedrock contour lines by the Yumenoshima explosion tests (Shima et al.,1976) and the geological contour lines of the bottom of the Quaternary layer by Kakimi et al.,1973 are used to investigate the 3D wave propagation characteristics of the Kanto basin. These two irregular boundaries lead to a 3D subsurface structure consisting of two sedimentary layers whose shear wave velocities are 0.7km/s and 1.3km/s on a bedrock with a shear velocity of 2.9km/s (ref.to Table1).

Figure 9 shows the contour lines of the phase velocities of the fundamental mode of the Love wave for 8s. Figure 10 shows those of the group velocities. These figures are obtained from the dispersion curves of the Love wave based on the local structures at all grid points (in this study, 3.6km by 3.2km). It is found from these figures that the phase and group velocities are lowest at the interior part of the Tokyo Bay and that there is a barrier with a steep velocity gradient, i.e. the contour lines are dense, behind the low velocity zone. This barrier may reflect the surface waves. Another barrier is recognized in the mountain area in the west part of the contour map. This barrier may deflect the wave propagation path of the surface wave.

It is noted that the depth of the bottom of the Quaternary layers of the 3D subsurface structure is not consistent with the 2D structure in Figure 4.

4.2 *Numerical methods and analytical model*

To examine the surface wave propagation characteristics, taking into account 3D subsurface irregularities of a large-scale basin, the authors have developed a simplified 3D-FEM (Toshinawa and Ohmachi,1990) to reduce the computational effort. To cope with the propagation of the Love wave in this study, the vertical degree of freedom at each nodal point of a prism element is neglected, but the remaining two horizontal degrees of freedom are taken into account. The linear combination of the modes of the Love wave in the local subsoil can be adopted as an interpolation function in the vertical direction for each prism element. The used prism element in this study is based on the acoustic wave equation for a shear wave. Although the mode is frequency dependent and mode coupling occurs in general, only the fundamental mode shape at a specific frequency is used in each element for the narrow-banded incident waves. The time domain analysis based on e.g. the central difference approximation is then applied.

The analytical model is a rectangle with 10200 triangular prism elements and 5246 nodal points for the bounded region of 60km by 85km, as shown in Figure 11. Viscous boundary conditions are applied at each model boundary, and the plane surface waves are used as input motions. The Gabor wavelet with a predominant period of 8s is used as the input wave for the normalized velocity in the x-direction. Figure 12 shows the results of the kinematic ray tracing of the Gaussian Beam Method (Yomogida et al.,1985) for the plane wave incidence based on the phase velocity contour in Figure 9.

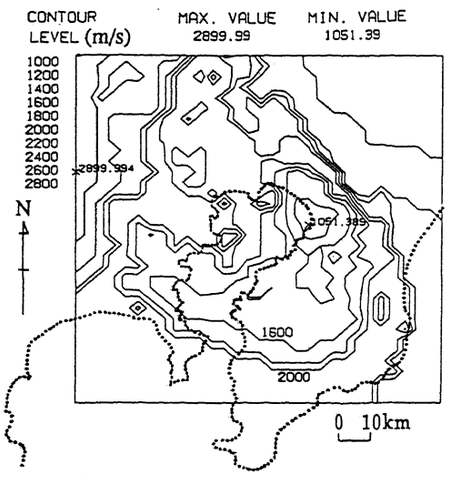

Figure 9. Contour map of phase velocities of fundamental mode of the Love wave for the period of 8 seconds

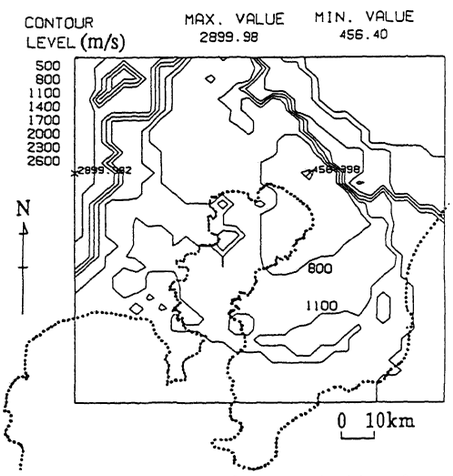

Figure 10. Contour map of group velocities of fundamental mode of the Love wave for the period of 8 seconds

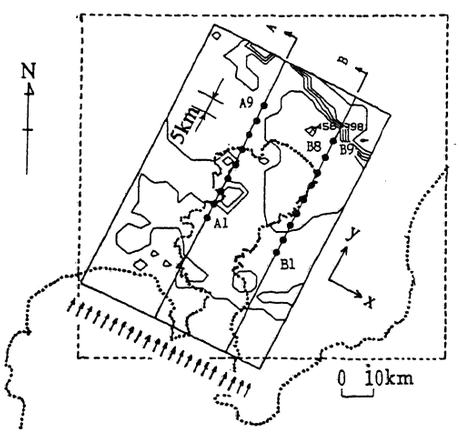

Figure 11. Simplified 3D-FEM model (3D-Model) for incident plane wave

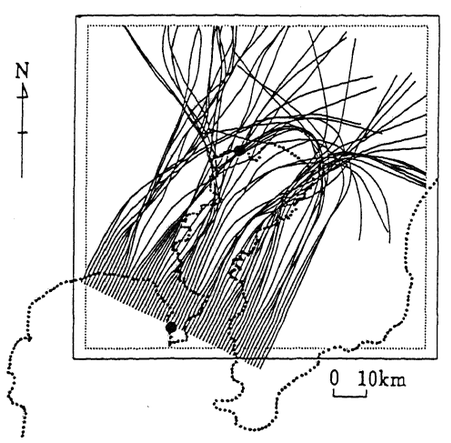

Figure 12. Kinematic ray tracing for incident plane wave (Fundamental mode of the Love wave at a period of 8.0 seconds)

4.3 *Results and discussions*

Figures 13 and 14 show the synthetic waveforms in the interior part of the Tokyo Bay along the specified lines A and B of 3D-Model in Figure 11. Line A is the line along the west side of the bay including the point at KOT(A6). Line B is the line along the east side of the bay. In these figures, waveforms in the x- and y-directions (ref.to Figure 11) are compared and the latter waveforms prove the deflection of the propagating surface waves due to the 3D irregularity of the basin. It is recognized that the amplitudes of the synthetic waveforms along line A are rather smaller than those along line B in the interior part of the bay. These results are reasonable judging from the phase and group velocity contour maps. The waveform at A6 corresponding to KOT is not amplified by the used geological structure as is seen in the observation records. This contradiction may be because the used Quaternary bottom by Kakimi et al.,1973 is rather shallower along the line A than in the section shown in Figure 4. However,the waveforms along the line B are strongly amplified at the points from B6 to B9, which correspond to the region where the rays are focused, as shown in Figure 12. The wave group propagates with a specific group velocity, as shown in Figure 14. The reflected wave due to the described barrier is clearly recognized.

To compare the results taking into account the 3D irregularity with those of the 2D sections, the

simplified 2D analysis based on the same assumption as the simplified 3D analysis is performed. The results are shown in Figures 15 and 16 for lines A and B. It is found that the 2D analysis yields a smaller amplification of the Love wave than the 3D analysis at the region of low group velocities, and that the phase of the reflected wave is clearer in the 2D analysis than in the 3D analysis.

To examine the wave propagation direction in the simplified 3D analysis, the orbits of the first major wave group are calculated at A1,B1, A7 and B7. Those of the reflected waves are also calculated at A7 and B7. The obtained orbits are shown in Figure 17. The propagation direction of each wave group is also indicated by an arrow in this figure. It is found from this figure that the orbits at A1 and B1 are flat and perpendicular to the propagation direction, but that the orbits of the first wave group at A7 and B7 are not flat and are rather elliptic. This means that the waveforms at these points consist of waves with the different propagation paths, as is suggested from Figure 12. The principal axes of the orbits are consistent with the kinematic ray tracing. The particle orbits of the reflected waves may indicate the reflecting points.

It is noted that these orbits for the plane surface wave are not consistent with those of the observation records at KOT. To understand that the principal axes of the orbits change clockwise with time, the relation of the rays affecting the propagation paths between the radiation pattern of the Love wave from the source is considered. Figure 18 shows the kinematic ray tracing from the source. This figure also shows the radiation pattern based on a strike slip of vertical fault for the source of the earthquake. It is suggested from this figure that the weighting factor of the rays polarized north and passing through the west side of the Tokyo

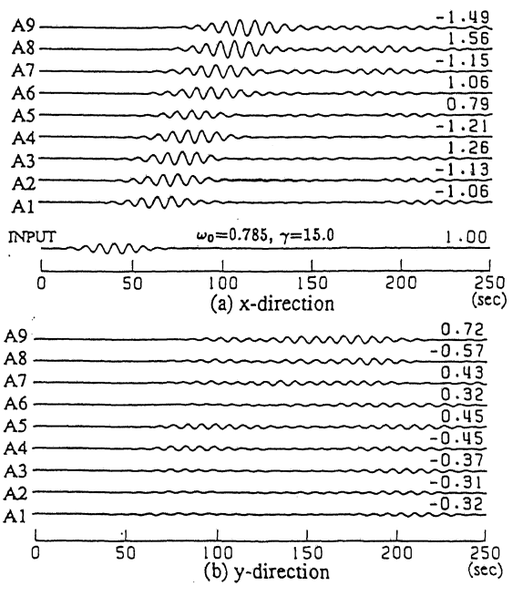

Figure 13. Synthetic waveforms on line A of 3D-Model.

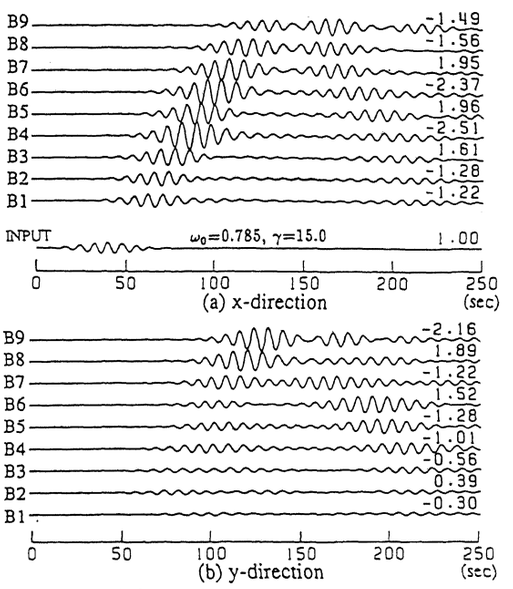

Figure 14. Synthetic waveforms on line B of 3D-Model.

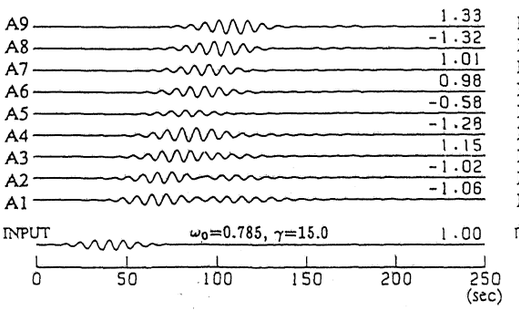

Figure 15. Synthetic waveforms by the simplified 2D-analysis based on the subsurface structure along line A of 3D-Model.

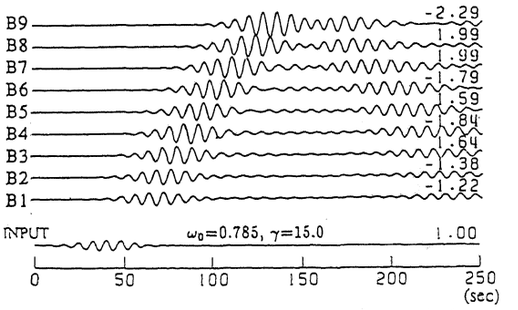

Figure 16. Synthetic waveforms by the simplified 2D-analysis based on the subsurface structure along line B of 3D-Model.

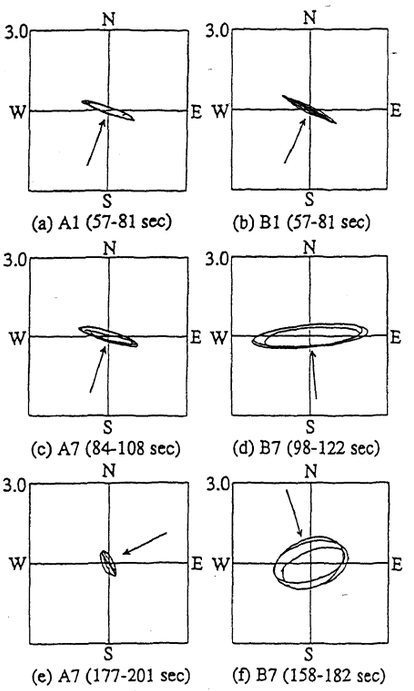

Figure 17. Particle orbits of the synthetic waves.

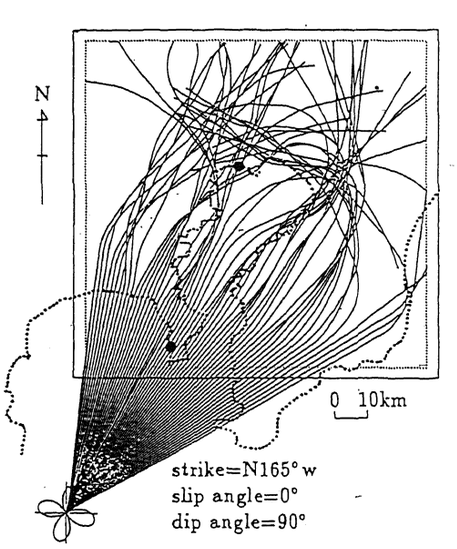

Figure 18. Kinematic ray tracing for the Feb.20, 1990 Near Izu-Oshima Earthquake (Fundamental mode of Love wave at a period of 8.0 seconds)

Bay is larger than that of the rays polarized in the north-east direction. This may explain the characteristics of the orbits of the observation records.

5 CONCLUDING REMARKS

Concluding remarks are as follows.
(1) The 2D analysis using the hyper-element method shows that the first major phase of the observation records is simulated well using the section of the geological structure, but the continued phases are not expressed, suggesting that the latter phases are affected by the 3D structure.
(2) The simplified 3D-FEM can be applied efficiently in computation to the wave propagation problem of a large scale basin.
(3) It is found that the consideration of the 3D irregular structure is important in estimating the long-period ground motion due to surface waves.
(4) The obtained 3D wave propagation characteristics in the basin may depend on the used subsurface structure and those are consistent with the information of the ray tracing.
(5) It is suggested that consideration of the radiation pattern from the source may be important as well as the identification of the actual 3D structure, especially the bottom of the Quaternary layers.

6 ACKNOWLEDGEMENT

The authors gratefully thank Dr. K. Kudo of the Earthquake Research Institute of the University of Tokyo who provided us with the valuable observation records of the Abratsubo site. They also thank Prof. E.Shima, Prof. Emeritus of the University of Tokyo, presently an advisor of Kajima Corporation, for his helpful advice on the geological structure of the Kanto basin.

REFERENCES

Cerveny, V. 1983. Synthetic body wave seismograms for laterally varying layered structure by Gaussian Beam Method. Geophy. J. R. Astron.Soc., 73, 389-426.
Kakimi,T, et al. 1973. Neotectonic Map of Tokyo. Geological Survey of Japan.
Kausel,E. and J.M.Rosset.1977. Semi-analytical hyper-element for layered strata, J. Eng. Mech. Div., EM4, 569-588.
Kudo,K. 1978. Contribution of surface waves to strong ground motions. Proc. 7th WCEE,2,499-506.
Motosaka,M. 1990. Analytical investigation of diffracted surface wave generated in a sedimentary basin. Proc. 18th Symposium on Ground Vibrations.
Niwa,M., et al.1990. Earthquake ground motion characteristics in Tokyo bay area, Part1. Summary of technical papers of annual meeting of AIJ,347-348.
Shima,E.,et al.,1976. On the base rock of Tokyo 1 & 2. Bull. Earthq. Res. Inst.,51,1-11 & 45-61.
Toshinawa,T. and T.Ohmachi,1990. Impulsive response of a surface layer analyzed by 3-D finite element methods. Proc. of 8JEES,1,349-354.
Yomogida,K. and K. Aki, 1985. Waveform synthesis of surface wave in a laterally heterogeneous earth by Gaussian Beam Method. J. Geophy. Res.,90,7665-7688.